Proc. Natl. Acad. Sci. U.S.A. **92**, 4947 (1995).
23. The expression and purification of recombinant human FKBP12 (*19*) and the FRB domain of human FRAP (*22*) have been described. Crystals of FKBP12-rapamycin-FRB were grown in 2 to 3 weeks at room temperature from hanging drops prepared from FKBP12 [10 mg/ml, in 10 mM tris-HCl (pH 8.0)], two equivalents of rapamycin (in methanol), and one equivalent of FRB [10 mg/ml, in 50 mM tris-HCl (pH 8.0)]. The well solution contained 20% (w/v) polyethylene glycol 8000, 10% methypentanediol, and 10 mM tris-HCl (pH 8.5). The rod-shaped crystals are orthorhombic, space group $P2_12_12_1$ with cell constants a = 44.63, b = 52.14, and c = 102.53 Å, and contain one ternary complex in the asymmetrical unit.
24. Data to a resolution of 2.7 Å (43,447 measurements of 6920 unique reflections, 98.5% complete, R_{sym} = 0.071) were collected from a crystal of dimensions 0.3 mm by 0.2 mm by 0.1 mm with the use of a San Diego multiwire area detector on a Rigaku RU-200 rotating anode x-ray source. Experimental phases were obtained from MR and SIRAS. MR with X-PLOR [A. T. Brünger, J. Kuriyan, M. Karplus, *Science* **235**, 458 (1987)] and the FKBP12-rapamycin model (*19*) yielded a clear solution, but the resulting electron density map was noisy. A mercury derivative was prepared (2 mM $HgCl_2$, overnight), and the two heavy atom sites were refined with PHASES [W. Furey and S. Swaminathan, *ACA Abstr.* **18**, 73 (1990)]. Anomalous dispersion measurements were included in this data set and 16 cycles of solvent flattening were applied (PHASES). The resulting electron density map clearly showed the four-helix–bundle architecture of FRB. The FKBP12-rapamycin portion of the structure was well defined in the initial electron density map, and minor changes in the backbone of the 30s loop and some side chains were sufficient to fit the model. For the FRB portion, most of a polyalanine chain could be traced for the helical regions of the initial map. After several cycles of positional refinement (X-PLOR), loop regions could also be traced and the side chains assigned. CHAIN [J. S. Sack, *J. Mol. Graphics* **6**, 244 (1988)] was used for model fitting and building the structure. A total of 95 residues in the FRB domain of FRAP (three residues in the NH_2-terminal and two residues in the COOH-terminal regions showed no electron density and were not included), all residues of FKBP12, all atoms of rapamycin, and 23 water molecules were included in the final model. FRB residues are numbered according to FRAP numbering. The current R factor is 0.193 (R_{free} = 0.299) for data from 8 to 2.7 Å. The root-mean-square deviations of bond lengths and bond angles are 0.008 Å and 1.48°, respectively. The average temperature factors for all atoms and main chain atoms are 17.0 and 14.7 Å^2, respectively.
25. N. L. Harris, S. R. Presnell, F. E. Cohen, *J. Mol. Biol.* **236**, 1356 (1994).
26. F. Lederer, A. Glatigny, P. H. Bethge, H. D. Bellamy, F. S. Mathews, *ibid.* **148**, 427 (1981).
27. J. A. Findlay and L. Radics, *Can. J. Chem.* **58**, 579 (1980).
28. X. F. Zheng, D. Fiorentino, J. Chen, G. R. Crabtree, S. L. Schreiber, *Cell* **82**, 121 (1995).
29. M. C. Lorenz and J. Heitman, *J. Biol. Chem.* **270**, 27531 (1995).
30. V. M. Rivera *et al.*, *Nature Med.*, in press.
31. M. Carson, *J. Mol. Graphics* **5**, 103 (1987).
32. A. C. Wallace, R. A. Laskowski, J. M. Thornton, *Prot. Engin.* **8**, 127 (1995).
33. A. Nicholls, K. Sharp, B. Honig, *GRASP Manual* (Columbia Univ. Press, New York, 1992).
34. We thank S. Ealick, J. Liang, and R. Gillilan for discussions. The Cornell work was funded in part by USPHS grant CA59021 (to J.C.) and the Harvard work by an Irvington Institute Fellowship (to J.C.) and USPHS grant GM38625 (to S.L.S.). S.L.S. is a Howard Hughes Medical Institute Investigator. Atomic coordinates have been deposited in the Protein Data Bank under the accession number 1FAP.

15 March 1996; accepted 15 May 1996

Long-Term Lymphohematopoietic Reconstitution by a Single CD34-Low/Negative Hematopoietic Stem Cell

Masatake Osawa,* Ken-ichi Hanada, Hirofumi Hamada, Hiromitsu Nakauchi†

Hematopoietic stem cells (HSCs) supply all blood cells throughout life by making use of their self-renewal and multilineage differentiation capabilities. A monoclonal antibody raised to the mouse homolog of CD34 (mCD34) was used to purify mouse HSCs to near homogeneity. Unlike in humans, primitive adult mouse bone marrow HSCs were detected in the mCD34 low to negative fraction. Injection of a single mCD34$^{lo/-}$, c-Kit$^+$, Sca-1$^+$, lineage markers negative (Lin$^-$) cell resulted in long-term reconstitution of the lymphohematopoietic system in 21 percent of recipients. Thus, the purified HSC population should enable analysis of the self-renewal and multilineage differentiation of individual HSCs.

CD34 is a marker of human HSCs, and all colony-forming activity of human bone marrow (BM) cells is found in the CD34-positive fraction (*1*). Clinical transplantation studies that used enriched CD34$^+$ BM cells also indicated the presence of HSCs with long-term BM reconstitution ability within this fraction (*2*). After isolation of the human CD34 gene, the mouse homolog (mCD34) was isolated by cross-hybridization (*3*). To examine the expression and function of mCD34, we raised a monoclonal antibody (mAb), 49E8 [rat immunoglobulin G2a (IgG2a)], to mCD34 by immunizing rats with a glutathione-S-transferase (GST)–mCD34 fusion protein. This mAb stained BaF3 cells transfected with a full-length mCD34 cDNA but not mock-transfected cells (*4*). Murine cell lines such as PA6, NIH 3T3, M1, and DA1, shown by reverse transcriptase–polymerase chain reaction (RT-PCR) to contain mCD34 mRNA, were also stained by this mAb, indicating that 49E8, although specific for a GST-mCD34 fusion protein, could also recognize the native form of mCD34 as expressed on various cell types (*4*).

We next examined adult mouse BM for expression of mCD34. Four-color fluorescence-activated cell sorter (FACS) analysis was done after sequential staining of BM cells with a combination of lineage-specific mAbs to CD4, CD8, B220, Gr-1, Mac-1, and TER119, and then a mixture of mAbs to c-Kit (ACK-2), Ly6A/E (Sca-1), and mCD34 (*5*). Monoclonal antibody 49E8 reacted with 2.5 ± 0.5% (mean ± SD) of total BM cells, with most of the positive cells occurring in the Lin$^-$ fraction (Fig. 1A). More than 90% of the c-Kit$^+$ Sca 1$^+$ Lin$^-$ cells previously shown to contain primitive HSCs (*6*) stained brightly with 49E8, whereas the remainder were low to negative (Fig. 1B). The frequency of mCD34$^+$ c-Kit$^+$ Sca-1$^+$ Lin$^-$ cells and mCD34$^-$ c-Kit$^+$ Sca-1$^+$ Lin$^-$ cells among total nucleated BM cells was 0.073 ± 0.028% (mean ± SD, n = 5) and 0.004 ± 0.003% (mean ± SD, n = 5), respectively.

To determine whether mouse HSCs express mCD34, we sorted subpopulations by FACS and examined their stem cell activity. Within the c-Kit$^+$ Sca-1$^+$ Lin$^-$ population, the frequency of interleukin-3 (IL-3)–dependent colony-forming unit culture (CFU-C) per 200 cells was 20.0 ± 3.9% (mean ± SD, n = 8) (*7*) for mCD34$^+$ cells but only 0.16 ± 0.4% (mean ± SD, n = 8) in the CD34$^-$ fraction. Similarly, mCD34$^+$ cells contained 14.1 ± 3.4% (mean ± SD, n = 15) day 12 CFU spleen (CFU-S) per 200 cells, whereas in the mCD34$^-$ fraction this value was 1.6 ± 1.7% (mean ± SD, n = 15) (*8*). Thus, colony-forming activity was positively correlated with mCD34 expression among c-Kit$^+$ Sca-1$^+$ Lin$^-$ cells. When these cells were cultured in the presence of both IL-3 and stem cell factor (SCF), however, 80% of mCD34$^-$ c-Kit$^+$ Sca-1$^+$ Lin$^-$ cells formed large multilineage colonies (*7*).

For in vivo analyses, c-Kit$^+$ Sca-1$^+$ Lin$^-$ cells were fractionated into mCD34$^{lo/-}$ (Fr. 1), mCD34^{lo} (Fr. 2), and CD34$^+$ (Fr. 3) subpopulations according to their mCD34 expression by FACS (Fig. 2A). Although 100 c-Kit$^+$ Sca-1$^+$ Lin$^-$ cells were sufficient to radioprotect a lethally irradiated mouse, injection of 300 cells from either the Fr. 1 or Fr. 3 subpopulation (Fig. 2A) alone showed poor radioprotective ability (*9*). When cells

M. Osawa and H. Nakauchi, Department of Immunology, Institute of Basic Medical Sciences and Center for Tsukuba Advanced Research Alliance, University of Tsukuba, Tsukuba Science-City, Ibaraki 305, Japan.
K.-i. Hanada and H. Hamada, Department of Molecular Biotherapy, Cancer Chemotherapy Center, Japanese Foundation for Cancer Research, Tokyo 170, Japan.

*Present address: KIRIN Pharmaceutical Research Laboratory, Gunma 371, Japan.
†To whom correspondence should be addressed.

of both fractions were transplanted together, however, both short-term and long-term engraftment was observed (9). These results support the hypothesis that there are two vital classes of engrafting cells: committed progenitor cells that provide initial engraftment and HSCs that are responsible for delayed but durable engraftment (*10*).

To further test this hypothesis, we used a competitive long-term reconstitution (CLTR) analysis of mouse strains congenic for different alleles of the Ly5 antigen on the C57BL/6 background. We determined the HSC activity by measuring long-term multilineage reconstitution of isolated donor (Ly5.1) cells, whereas minimum radioprotection was provided by congenic host (Ly5.2) BM Lin^- cells. Cells in the three fractions (Fig. 2A) were each examined for CLTR ability (*11*). As in Fig. 2B, $mCD34^+$ $c\text{-}Kit^+$ $Sca\text{-}1^+$ Lin^- cells revealed early but unsustained multilineage hematopoietic reconstitution, indicating that the cells in this fraction are capable of multilineage differentiation but not of self-renewal (Fig. 2B). In contrast, delayed but long-term multilineage reconstitution was observed after transplantation of $mCD34^{lo/-}$ $c\text{-}Kit^+$ $Sca\text{-}1^+$ Lin^- cells (Fig. 2B). Thus, radioprotection does not reflect true HSC activity, and primitive HSCs with self-renewal capacity can be clearly separated from (i) IL-3–dependent CFU-C, (ii) day 12 CFU-S, and (iii) the cells that retain multilineage differentiation capacity but have lost self-renewal potential.

Using a polyclonal antibody against mCD34, Krause *et al.* reported that HSCs with the ability to repopulate BM of lethally irradiated mice for 60 days were enriched in the $mCD34^+$ population (*12*). This result, however, does not definitively exclude the presence of HSCs in the $mCD34^-$ population because Krause *et al.* (*12*) did not inject rescue cells along with the $mCD34^-$ cells to examine long-term repopulating ability. In addition, their $CD34^+$ fraction could have contained Lin^+ cells because they obtained these cells by single-color cell sorting from total BM mononuclear cells, whereas in our experiments $CD34^+$ cells were Lin^-. Thus, HSC activity of the $CD34^+$ cells observed by Krause *et al.* could have been due to the presence of Lin^+ stem cells reported elsewhere (*13*).

Given, however, that native mCD34 is heavily glycosylated, it was possible that the ability of 49E8 to recognize its epitope on cells with HSC activity was blocked by an unusual sugar modification. To rule out this possibility, we examined the cells in three fractions of the $c\text{-}Kit^+$ $Sca\text{-}1^+$ Lin^- cells (Fig. 2A) for the presence of mCD34 transcripts. Analysis by RT-PCR revealed a difference in the levels of mCD34 mRNA among these three fractions corresponding to the differences observed with the antibody (Fig. 2C) (*14*). Thus, on the basis of the expression of mCD34, HSCs are distinguishable from progenitors cells that have multilineage differentiation potential but lack self-renewal capability.

We further assessed the purity of HSCs by injecting a graded number of FACS-purified $mCD34^{lo/-}$ $c\text{-}Kit^+$ $Sca\text{-}1^+$ Lin^- cells from Ly5.1 BM cells into lethally irradiated Ly5.2 congenic hosts, along with 500 Ly5.2 BM-derived $mCD34^+$ $c\text{-}Kit^+$ $Sca\text{-}1^+$ Lin^- cells to provide short-term (but not long-term) radioprotection (Table 1). Injection of a single $mCD34^{lo/-}$ $c\text{-}Kit^+$ $Sca\text{-}1^+$ Lin^- cell reconstituted the lymphohematopoietic system for more than 3 months in 21% of recipients. Approximately 85% of the cells of both myeloid and lymphoid lineages in the peripheral blood of the survivors were of donor origin. Furthermore, in the analysis of the recipients of the $mCD34^{lo/-}$ $c\text{-}Kit^+$ $Sca\text{-}1^+$ Lin^- cell, we detected both $mCD34^{lo/-}$ and $mCD34^+$ cells of donor origin in the host's BM, demonstrating the expansion of a $mCD34^{lo/-}$ HSC and differentiation into $mCD34^+$ progenitor cells. Secondary transfer of donor-derived $mCD34^{lo/-}$ $c\text{-}Kit^+$ $Sca\text{-}1^+$ Lin^- cells resulted in repopulation of lethally irradiated congenic host's BM for up to 4 months (9).

Smith *et al.* reported a similar experiment

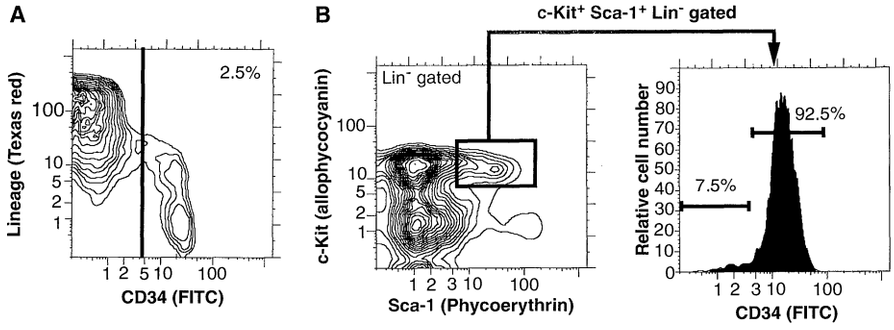

Fig. 1. Flow cytometric analysis of mCD34 expression on murine BM cells. (**A**) Staining profile of lineage markers versus mCD34 on total BM cells. (**B**) Expression of mCD34 on $c\text{-}Kit^+$ $Sca\text{-}1^+$ Lin^- cells. A gate was set on $c\text{-}Kit^+$ $Sca\text{-}1^+$ Lin^- cells (left), and the expression of mCD34 on those cells was examined. Fluorescence histogram (right) shows mCD34 staining profile of the gated, stem cell–enriched fraction. Of $c\text{-}Kit^+$ $Sca\text{-}1^+$ Lin^- cells, 92.5% stained brightly with 49E8, and the rest were negative.

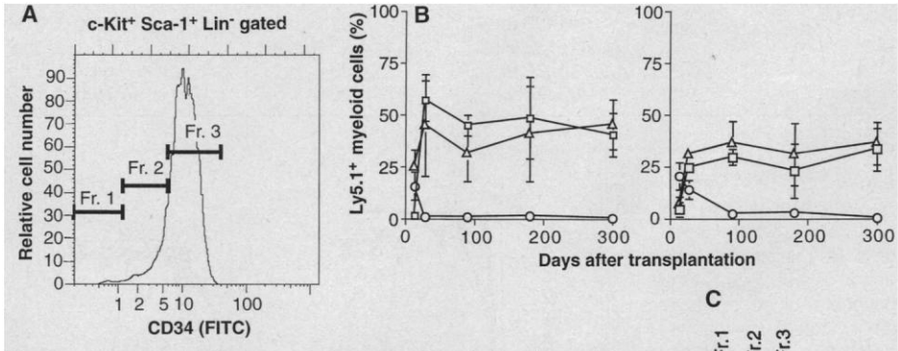

Fig. 2. In vivo analysis of hematopoietic stem cell activity in subpopulations of $c\text{-}Kit^+$ $Sca\text{-}1^+$ Lin^- cells fractionated by mCD34 expression. (**A**) Separation of $c\text{-}Kit^+$ $Sca\text{-}1^+$ Lin^- cells by the expression level of mCD34. Fluorescence histogram shows anti-mCD34 staining of $c\text{-}Kit^+$ $Sca\text{-}1^+$ Lin^- cells. By FACS analysis, $c\text{-}Kit^+$ $Sca\text{-}1^+$ Lin^- cells were sorted into three subpopulations: $mCD34^{lo/-}$, $mCD34^{lo}$, and $mCD34^+$ (Fr. 1, Fr. 2, and Fr. 3, respectively) as indicated by the horizontal lines. (**B**) Competitive long-term repopulation abilities of isolated subpopulations. Donor ($Ly5.1^+$)-derived cells were detected in the peripheral blood of recipient mice transplanted with 100 Fr. 1 (□) or Fr. 2 cells (△) or 500 Fr. 3 cells (○). The percentage of donor-derived cells within myeloid cells ($Mac\text{-}1^+$ and $Gr\text{-}1^+$) and lymphoid cells ($Thy\text{-}1^+$ or $B220^+$) was measured at various time points after transplantation. The data are shown as the mean ± SD of three independent experiments with five to eight animals per trial. (**C**) Expression of mCD34 and HPRT genes within isolated subpopulations was analyzed by RT-PCR. One thousand Fr. 1, Fr. 2, or Fr. 3 cells were sorted and subjected to RT-PCR analysis. RT-PCR–amplified products from mCD34 gene (upper panel) and from HPRT gene as control (lower panel) were electrophoresed, transferred to a nylon membrane, and probed with internal oligonucleotides.

in which Thy-1^{lo} Lin$^-$ Sca-1$^+$ cells were used (*15*). These cells are present in BM at a frequency of 0.02 to 0.05%, suggesting that this population is nearly 10 times less enriched for HSCs than is the mCD34$^{lo/-}$ c-Kit$^+$ Sca-1$^+$ Lin$^-$ population, which we find occurs at a frequency of 0.004%. Similarly, these authors observed lymphohematopoietic reconstitution in only 2 (0.7%) out of 280 recipients of single FACS-sorted cells at 8 weeks after transplantation (*15*). In our experiment, 21% of the animals reconstituted with a single mCD34$^{lo/-}$ c-Kit$^+$ Sca-1$^+$ Lin$^-$ cell maintain lymphohematopoiesis at high levels for more than 3 months. This result suggests a greater purity of HSCs in our population compared with that defined by Thy-1 expression. The representation of HSCs in our population is almost certain to be much higher than 21% because, in our single-cell injection, all the HSCs are unlikely to be successfully transplanted and seeded in a suitable microenvironment.

Among nine survivors of the single-cell reconstitution, one mouse died of unknown causes 4 months after transplantation, and six recipients showed a degree of reconstitution such that more than 50% of both myeloid and lymphoid cells in the peripheral blood were derived from the injected donor stem cell throughout our observation period of up to 10 months (Fig. 3, A and B). Three recipients showed a decrease in myeloid or lymphoid reconstitution 7 months after transplantation (Fig. 3A). The difference in the long-term lymphohematopoietic reconstitution in each individual HSC may suggest a variability in HSCs with respect to self-renewal potential as well as multilineage differentiation potential.

Our present observations are in agreement with a recent report showing near normal adulthood hematopoiesis in mCD34 knockout mice (*16*). Our findings have potential implications for the prospect of purification and expansion of human HSCs on the basis of CD34 expression as the sole criterion. Several studies, including allogenic and xenogenic transplantation, show the presence of HSCs in the CD34$^+$ fraction (*2*, *17*). Human and mouse could differ in the expression of CD34 antigen. However, without an appropriate assay system, phenotypic definition of HSCs should be made only after careful experimental studies.

Table 1. Graded number of CD34$^{lo/-}$ c-Kit$^+$ Sca-1$^+$ Lin$^-$ cells (Fr. 1 cells in Fig. 2A) isolated from C57BL/6-Ly5.1 mice were injected into lethally irradiated congenic (C57BL/6-Ly5.2) mice, together with 500 CD34$^+$ c-Kit$^+$ Sca-1$^+$ Lin$^-$ cells (Fr. 3 cells in Fig. 2A) of Ly5.2 origin. At 3 months after transplantation, the percentage of donor (Ly5.1$^+$)-derived myeloid (Mac-1$^+$ and Gr-1$^+$) cells and lymphoid (Thy-1$^+$ and B220$^+$) cells in the peripheral blood of recipient animals was analyzed. The recipients that survived for 3 months and in whose peripheral blood Ly5.1$^+$ cells were detected were scored as reconstituted mice. The results are shown as the mean ± SD.

Reconstitution ability of CD34$^{lo/-}$ c-Kit$^+$ Sca-1$^+$ Lin$^-$ cells			
No. of mCD34$^{lo/-}$ c-Kit$^+$ Sca-1$^+$ Lin$^-$ cells injected	No. of mice reconstituted/ tested (%)	Chimerism (% Ly5.1$^+$ cells)	
		Myeloid (%)	Lymphoid (%)
1	9/41 (21.9)	87.1 ± 11.9	59.1 ± 20.5
2	5/21 (23.8)	92.4 ± 1.34	64.0 ± 6.36
5	9/17 (52.9)	95.8 ± 4.11	66.1 ± 18.2
10	10/11 (90.9)	99.3 ± 1.09	64.7 ± 21.5
20	4/4 (100)	98.6 ± 5.3	75.6 ± 15.8

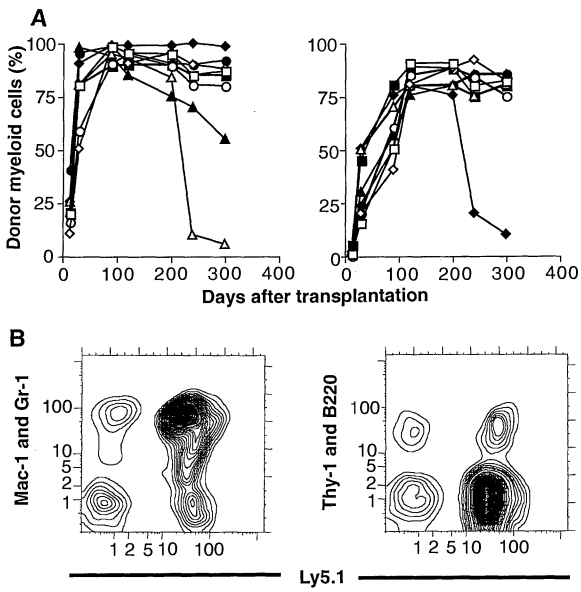

Fig. 3. Long-term lymphohematopoietic reconstitution by single mCD34$^{lo/-}$ c-Kit$^+$ Sca-1$^+$ Lin$^-$ cells. (**A**) Long-term observation of donor-derived (Ly5.1$^+$) cells in the peripheral blood of recipient mice reconstituted with a single mCD34$^{lo/-}$ c-Kit$^+$ Sca-1$^+$ Lin$^-$ cell (Table 1). Each data point represents the frequency of donor-derived cells in the peripheral blood of an individual recipient. (**B**) Analysis of lymphohematopoietic reconstitution 10 months after transplantation. The cells from the peripheral blood were stained with donor-specific Ly5.1-FITC, myeloid-specific PE–Mac-1 and PE-Gr-1, and lymphoid-specific APC–Thy-1 and APC-B220 and analyzed by FACS. A representative analysis is shown in which chimerism is ~82%.

REFERENCES AND NOTES

1. C. I. Civin *et al.*, *J. Immunol.* **133**, 157 (1984); C. M. Baum, I. L. Weissman, A. S. Tsukamoto, A. M. Buckle, B. Peault, *Proc. Natl. Acad. Sci. U.S.A.* **89**, 2804 (1992).
2. G. E. Tjonnfjord, R. Steen, O. P. Veiby, W. Friedrich, T. Egeland, *Blood* **84**, 3584 (1994); D. B. Kohn *et al.*, *Nature Med.* **1**, 1017 (1995).
3. J. Brown, M. F. Greaves, H. V. Molgaard, *Int. Immunol.* **3**, 175 (1991); J. Suda *et al.*, *Blood* **79**, 2288 (1992).
4. M. Osawa, K.-i. Hanada, H. Hamada, H. Nakauchi, unpublished results.
5. The BM cell suspension was prepared from C57BL/6 mice (8 to 10 weeks old) and stained with biotinylated antibodies to lineage (anti-lineage) markers (Mac-1, Gr-1, B220, CD4, CD8, and TER119), fluorescein isothiocyanate (FITC)–mCD34 (49E8), phycoerythrin (PE)–Sca-1 (E13-161.7; Pharmingen), and allophycocyanin (APC)–c-Kit (ACK-2). Biotinylated antibodies were detected with Texas red–streptavidin (Gibco-BRL). Stained cells were suspended in staining medium [phosphate-buffered saline, 0.05% NaN_3, and 3% fetal bovine serum (FBS)] containing propidium iodide (PI) (1 μg/ml) and analyzed on a FACS Vantage (Becton Dickinson). Residual erythrocytes, debris, doublets, and dead cells were excluded by forward scatter, side scatter, and PI gatings as described (6).
6. S. Okada *et al.*, *Blood* **80**, 3044 (1992); M. Osawa *et al.*, *J. Immunol.* **156**, 3207 (1996).
7. Bone marrow cells were obtained from the tibias and femurs of C57BL/6 mice. The suspension was overlaid with sodium metrizoate (Nycomed; Oslo, Norway) solution (1.086 g/ml) and centrifuged at 400*g* for 15 min. The low-density cells were harvested and incubated with biotinylated anti-lineage markers (Mac-1, Gr-1, B220, CD4, CD8, and TER119). Lin$^+$ cells were depleted with streptavidin-conjugated magnetic beads (PerSeptive Diagnostics, Cambridge, MA). The lineage-depleted cell population was then collected and incubated with FITC–anti-mCD34, PE–Sca-1, Texas red–streptavidin, and APC–anti–c-Kit. Stained cells were sorted with a Clone Cyt (Becton Dickinson) apparatus to deposit the required number of cells into 96-well microtiter plates. Two hundred mCD34$^-$ or mCD34$^+$ cells within the c-Kit$^+$ Sca-1$^+$ Lin$^-$ population were sorted and subjected to in vitro colony assay. The sorted cells were plated in 1.0% methylcellulose in α-medium (Flow Laboratories, North Ryde, Australia) supplemented with 30% FBS, 1% bovine serum albumin (BSA), 2-mercaptoethanol (10^{-4} mol/liter), and recombinant mouse IL-3 (20 ng/ml) or IL-3 plus stem cell factor (SCF, 20 ng/ml). The colonies that were formed by the stimulation of IL-3 or IL-3 plus SCF were counted after 14 days of incubation at 37°C in a humidified atmosphere of 5% CO_2.
8. Bone marrow cells were stained and sorted as described (7). Two hundred mCD34$^-$ c-Kit$^+$ Sca-1$^+$ Lin$^-$ cells or mCD34$^+$ c-Kit$^+$ Sca-1$^+$ Lin$^-$ cells were injected intravenously into lethally irradiated mice [9.5 gray (Gy) total body irradiation]. The spleens were removed on day 12 after injection and fixed in Bouin's solution, and macroscopically visible spleen colonies were counted.
9. M. Osawa and H. Nakauchi, data not shown.
10. R. J. Jones, J. E. Wagner, P. Celano, M. S. Zicha, S. J. Sharkis, *Nature* **347**, 188 (1990).

11. Bone marrow c-Kit$^+$ Sca-1$^+$ Lin$^-$ cells were fractionated according to the extent of mCD34 expression. One hundred Fr. 1 or Fr. 2 cells or 500 Fr. 3 cells (Fig. 2A) from Ly5.1 mice were sorted into a well containing 2×10^4 lineage-depleted BM cells from C57BL/6-Ly5.2 mice. In a preliminary experiment, we determined that 2×10^4 lineage-depleted BM cells were the minimum number of cells required for the survival of lethally irradiated recipients and reconstitution of their hematopoiesis. The cells in each well were collected and transferred into lethally irradiated C57BL/6-Ly5.2 mice. Several weeks to months after the transplantation, peripheral blood mononuclear cells were collected from the retro-orbital sinus and stained with FITC–anti-Ly5.1, PE–anti-myeloid (Mac-1 and Gr-1), and APC–anti-lymphoid (Thy1.2 and B220). The proportion of myeloid and lymphoid cells that originated from Ly5.1 cells was estimated by flow cytometry as described [S. Okada *et al.*, *Blood* **81**, 1720 (1993)].
12. D. S. Krause *et al.*, *Blood* **84**, 691 (1994).
13. M. Onishi *et al.*, *ibid.* **81**, 3217 (1993); J. P. Wineman *et al.*, *ibid.* **80**, 1717 (1992).
14. One thousand Fr. 1, Fr. 2, or Fr. 3 cells (Fig. 2A) were sorted and lysed in 50 μl of Isogen-LS (Nippon Gene, Tokyo). Total RNA was isolated according to the manufacturer's protocol. The first-strand cDNA reaction was carried out with 100 U of Molony murine leukemia virus reverse transcriptase (Gibco-BRL) in 20 mM tris-HCl (pH 8.4), 50 mM KCl, 2.5 mM $MgCl_2$, 0.5 mM deoxynucleoside triphosphate (dNTP), 10 mM DTT, and 0.25 μg of oligo(dT)$_{12-18}$. For the analysis of mCD34 and hypoxanthine phosphoribosyl transferase (HPRT) gene expression, the following specific primers were used to amplify fragments from one-half of the cDNAs obtained from each of the fractions: mCD34 [5′-ATGCAGGTCCACAGGGACACG-3′ and 5′-CTGTCCTGATAGATCAAGTAG-3′, generating a 221–base pair (bp) fragment]; and HPRT (5′-GCTGGTGAAAAGGACCTCTCG-3′ and 5′-GCAGATGGCCACAGGACTAGA-3′, generating a 258-bp fragment). PCR conditions were as follows: 20 mM tris-HCl (pH 8.4), 50 mM KCl, 1.5 mM $MgCl_2$, 0.2 mM dNTPs, 2.5 U of Ex Taq (Takara Ohtsu, Japan), and 50 pmol of each primer for 30 cycles (94°C, 30 s; 55°C, 30 s; 72°C, 45 s) followed by 5 min at 72°C in a Perkin-Elmer thermocycler. Each PCR product was electrophoresed through 2% agarose, transferred to a nylon membrane, and hybridized with a biotinylated internal oligonucleotide. Hybridized probes were detected with an ECL system (Amersham Life Sciences) according to the manufacturer's protocol.
15. L. G. Smith, I. L. Weissman, S. Heimfeld, *Proc. Natl. Acad. Sci. U.S.A.* **88**, 2788 (1991).
16. J. Cheng *et al.*, *Blood* **87**, 479 (1996).
17. E. F. Srour *et al.*, *ibid.* **82**, 3333 (1993).
18. We thank H. Kodama for discussion, T. Toyoshima for FACS operation, M. Ito for secretarial assistance, and C. Tarlinton for reading the manuscript. Supported by grants from Fujisawa Pharmaceutical, Uehara Memorial Foundation, The Ministry of Education, Science, and Culture, and the Agency for Science and Technology, Japan.

2 February 1996; accepted 29 April 1996

Regulation of Myosin Phosphatase by Rho and Rho-Associated Kinase (Rho-Kinase)

Kazushi Kimura, Masaaki Ito, Mutsuki Amano, Kazuyasu Chihara, Yuko Fukata, Masato Nakafuku, Bunpei Yamamori, Jianhua Feng, Takeshi Nakano, Katsuya Okawa, Akihiro Iwamatsu, Kozo Kaibuchi*

The small guanosine triphosphatase Rho is implicated in myosin light chain (MLC) phosphorylation, which results in contraction of smooth muscle and interaction of actin and myosin in nonmuscle cells. The guanosine triphosphate (GTP)–bound, active form of RhoA (GTP·RhoA) specifically interacted with the myosin-binding subunit (MBS) of myosin phosphatase, which regulates the extent of phosphorylation of MLC. Rho-associated kinase (Rho-kinase), which is activated by GTP·RhoA, phosphorylated MBS and consequently inactivated myosin phosphatase. Overexpression of RhoA or activated RhoA in NIH 3T3 cells increased phosphorylation of MBS and MLC. Thus, Rho appears to inhibit myosin phosphatase through the action of Rho-kinase.

Stimulation of smooth muscle and nonmuscle cells by specific agonists induces Ca^{2+} mobilization and activation of MLC kinase, which phosphorylates MLC and activates the myosin adenosine triphosphatase. This sequence of events results in contraction of smooth muscle (*1*) and interaction of actin and myosin for stress fiber formation in nonmuscle cells (*2*). However, because the cytosolic concentration of Ca^{2+} is not always proportional to the extent of MLC phosphorylation and contraction, an additional mechanism to regulate the Ca^{2+} sensitivity of both processes has been proposed (*3*). Because agonists induce MLC phosphorylation and contraction in permeabilized smooth muscle at fixed submaximal concentrations of Ca^{2+} in a GTP-dependent manner, a GTP binding protein is thought to regulate the receptor-mediated sensitization of MLC phosphorylation to Ca^{2+} (*4*). The small guanosine triphosphatase (GTPase) Rho is implicated in the enhancement of Ca^{2+} sensitivity of smooth muscle contraction by GTP (*5*). In permeabilized smooth muscle cells, the nonhydrolyzable GTP analog guanosine 5′-O-(3-thiotriphosphate) (GTP-γ-S) increases MLC phosphorylation at submaximal Ca^{2+} concentrations by inhibiting dephosphorylation of MLC, presumably by activating Rho (*6*). Rho exhibits both GDP (guanosine diphosphate) and GTP binding and GTPase activities (*7*). GTP·Rho presumably binds to specific targets and thereby exerts its biological functions, which include regulation of the formation of stress fibers and focal adhesions, cell motility, cell aggregation, and cytokinesis (*7*). We have identified two putative targets for Rho, p128 and p164 (*8*). The p128 protein is a serine-threonine kinase, known as protein kinase N (PKN) (*8*, *9*). The p164 protein is a serine-threonine kinase termed Rho-kinase (*10*). Activated Rho directly interacts with PKN and Rho-kinase, and stimulates their kinase activities (*8*, *10*).

To identify Rho targets other than PKN and Rho-kinase, we applied crude extracts of bovine brain membranes to glutathione-Sepharose (Pharmacia) affinity columns to which glutathione-S-transferase (GST), a GDP-bound GST-RhoA fusion protein (GDP·GST-RhoA), GTP-γ-S·GST-RhoA, GTP-γ-S·GST-RhoA^{A37}, GDP·GST-Rac1, or GTP-γ-S·GST-Rac1 was immobilized. RhoA^{A37} is structurally equivalent to H-Ras^{A35}, which has a mutation in the effector-interacting domain (substitution of threonine by alanine) (*7*, *11*). In addition to p128 and p164, a 138-kD protein (p138) was eluted from the GTP-γ-S·GST-RhoA affinity column, but not from the GST or GDP·GST-RhoA columns (Fig. 1A), indicating that p138 specifically interacted either directly or indirectly with the GTP-γ-S–bound form of GST-RhoA. The p138 protein was eluted from neither the GTP-γ-S·GST-RhoA^{A37} nor the GTP-γ-S·GST-Rac1 affinity columns.

The sequences of nine peptides derived from p138 were determined: RWIGSE, SLLQM, GYTEVL, ETLIIEPEK, DESPA, AYVAPTV, SLQGI, AQLHDTNMAL, and DENGALIRVIS (*12*). These sequences were almost identical to that of the 110-kD regulatory subunit of rat smooth muscle protein phosphatase 1M (*13*), which is a homolog of the myosin-binding subunit (MBS) of myosin phosphatase from chicken (*14*). We further confirmed that p138 is MBS by immunoblot analysis. The p138 protein was recognized by antibodies to MBS; an immunoreactive band was specifically detected in the eluate from the GTP-γ-S·GST-RhoA affinity column (Fig. 1B). Therefore, we concluded that p138

K. Kimura, M. Amano, K. Chihara, Y. Fukata, M. Nakafuku, K. Kaibuchi, Division of Signal Transduction, Nara Institute of Science and Technology, Ikoma 630-01, Japan.
M. Ito, B. Yamamori, J. Feng, T. Nakano, First Department of Internal Medicine, Mie University School of Medicine, Tsu 514, Japan.
K. Okawa and A. Iwamatsu, Central Laboratories for Key Technology, Kirin Brewery Company Limited, Yokohama 236, Japan.
*To whom correspondence should be addressed.